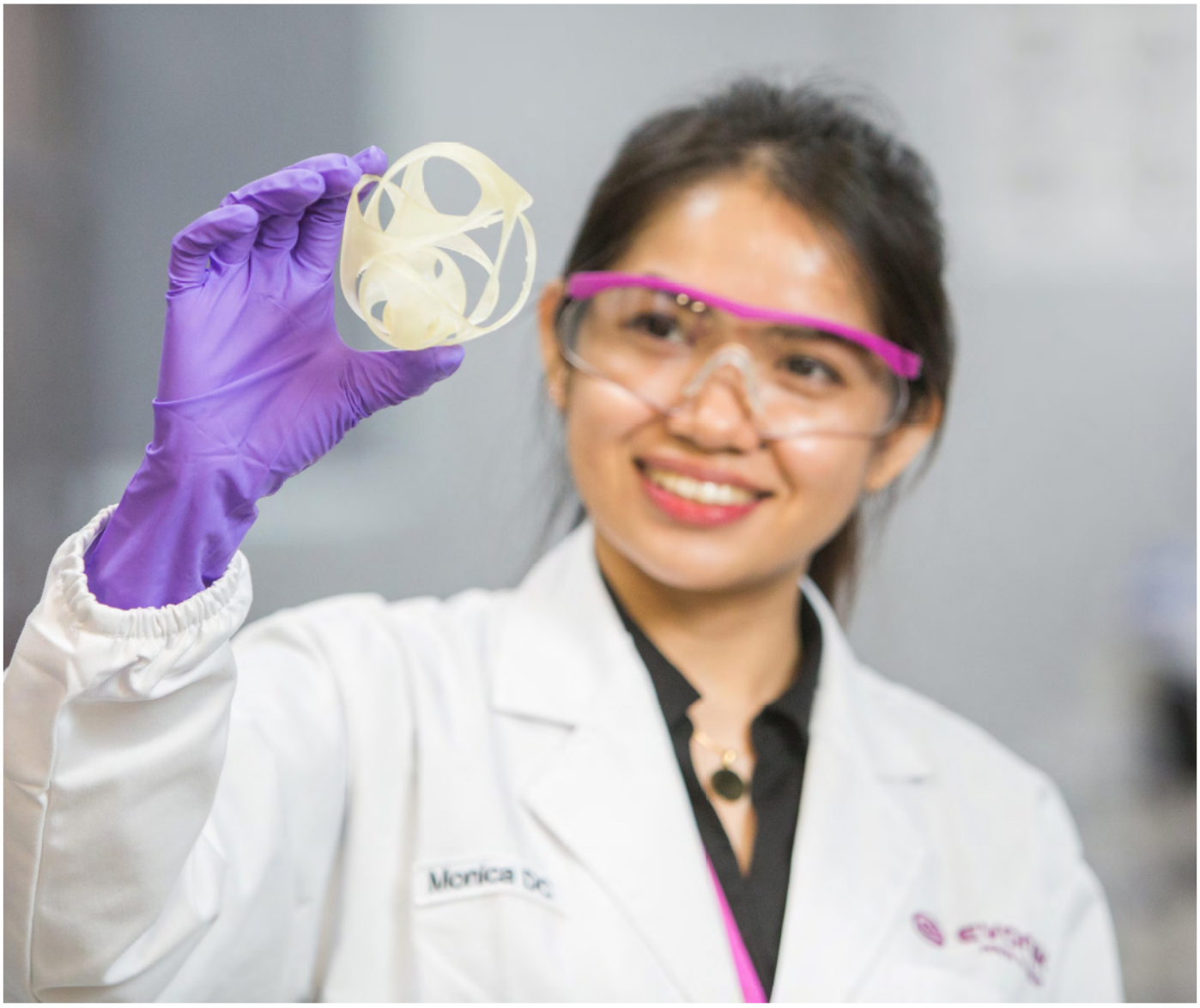

Pushing the boundaries of chemistry? It takes #HumanChemistry

Make your curiosity and talent as a chemist matter to the world with a specialty chemicals leader. Together, we combine cutting-edge science with engineering expertise to create solutions that answer real-world problems. Find out how our approach to technology creates more opportunities for growth, and see what chemistry can do for you at:

evonik.com/career

EVONIK
Leading Beyond Chemistry

ADVANCED FUNCTIONAL MATERIALS
www.afm-journal.de

On the Catalytic Activity of Sn Monomers and Dimers at Graphene Edges and the Synchronized Edge Dependence of Diffusing Atoms in Sn Dimers

Xiaoqin Yang, Huy Q. Ta, Huimin Hu, Shuyuan Liu, Yu Liu, Alicja Bachmatiuk, Jinping Luo, Lijun Liu, Jin-Ho Choi,* and Mark H. Rummeli**

In this study, in situ transmission electron microscopy is performed to study the interaction between single (monomer) and paired (dimer) Sn atoms at graphene edges. The results reveal that a single Sn atom can catalyze both the growth and etching of graphene by the addition and removal of C atoms respectively. Additionally, the frequencies of the energetically favorable configurations of an Sn atom at a graphene edge, calculated using density functional theory calculations, are compared with experimental observations and are found to be in good agreement. The remarkable dynamic processes of binary atoms (dimers) are also investigated and is the first such study to the best of the knowledge. Dimer diffusion along the graphene edges depends on the graphene edge termination. Atom pairs (dimers) involving an armchair configuration tend to diffuse with a synchronized shuffling (step-wise shift) action, while dimer diffusion at zigzag edge terminations show a strong propensity to collapse the dimer with each atom diffusing in opposite directions (monomer formation). Moreover, the data reveals the role of C feedstock availability on the choice a single Sn atom makes in terms of graphene growth or etching. This study advances the understanding single atom catalytic activity at graphene edges.

1. Introduction

Single-atom catalysts (SACs) have recently attracted interest in the fields of heterogeneous catalysis and electrocatalysis due to the enhancement in intrinsic activity and selectivity through optimized exposure of the active sites.[1–7] Downsizing metal nanoparticles into nanoclusters, and even single atoms, can evidently increase the catalytic activity and selectivity toward electrochemical reactions.[7–13] Recently, atoms at graphene edges have attracted significant interest for their catalytic potential, particularly with regards to their potential for the catalytic growth of sp^2 carbon (e.g., graphene) as well as their catalytic etching activity.[14–18] A catalytic process typically involves complex atomic-scale bond breaking and reforming events that are hard to resolve either spatially or temporally.

Dr. X. Yang, Dr. J. Luo, Prof. L. Liu
Scshool of Energy and Power Engineering
Xi'an Jiaotong University
No. 28, Xianning West Road, Xi'an, Shaanxi 710049, China
E-mail: ljliu@mail.xjtu.edu.cn

Dr. H. Q. Ta, Prof. A. Bachmatiuk, Prof. M. H. Rummeli
IFW Dresden
P.O. Box D-01171 Dresden, Germany

Dr. H. Hu, Dr. Y. Liu, Prof. J.-H. Choi, Prof. M. H. Rummeli
Soochow Institute for Energy and Materials Innovations
College of Physics
Optoelectronics and Energy
Collaborative Innovation Center of Suzhou Nano
Science and Technology
Key Laboratory of Advanced Carbon Materials and Wearable Energy
Technologies of Jiangsu Province
Soochow University
Suzhou 215006, China
E-mail: jhchoi@suda.edu.cn; mhr1@suda.edu.cn

Dr. S. Liu
Department of Physics
Research Institute for Natural Science, and Institute
for High Pressure at Hanyang University
Hanyang University
222 Wangsimni-ro, Seongdong-Ku, Seoul 04763, Republic of Korea

Prof. A. Bachmatiuk, Prof. M. H. Rummeli
Centre of Polymer and Carbon Materials
Polish Academy of Sciences
M. Curie-Sklodowskiej 34, Zabrze 41-819, Poland

Prof. A. Bachmatiuk
Łukasiewicz Research Network - PORT Polish Center
for Technology Development
ul. Stablowicka 147, Wrocław 54-066, Poland

Prof. M. H. Rummeli
Institute of Environmental Technology
VSB-Technical University of Ostrava
17. Listopadu 15, Ostrava 708 33, Czech Republic

The ORCID identification number(s) for the author(s) of this article can be found under https://doi.org/10.1002/adfm.202104340.

DOI: 10.1002/adfm.202104340

Aberration-corrected high-resolution transmission electron microscopy (HRTEM) provides a powerful tool with which to study the interactions between atoms and graphene, which is essential to understand their catalytic growth and etching activity and edge diffusion properties.[19,20] By employing HRTEM, the structure and dynamics of Au,[21] Fe,[15] Cu,[18] Cr,[16] Si,[17] and Pt[18,22] atoms at the edges of graphene have been studied through electron beam driven processes (and at times with additional heating). In the first such study using solely the imaging electron beam as a reaction driving system, Zhao et al. directly observed the diffusion and catalytic etching and growth roles of a single iron (Fe) atom at graphene edges through the removal and addition of C units, respectively.[15] A similar study, again by the Rümmeli group, investigated the behavior of single Chromium (Cr) atoms at graphene edges. Unlike the case for Fe atoms, Cr atoms showed a preference for the growth of graphene (since no etching activity was observed). The efficacy of a single Cr atom as a catalyst for sp^2 C growth as compared to a single Fe atom was further understood through supporting molecular dynamics calculations and showed the enhanced catalytic growth properties of Cr atoms could be attributed to differing energetics and kinetic stability as compared to Fe atoms.[16] Kano et al. explored the diffusion of individual Cu and Pt atoms along graphene edges, and they showed substitutional Cu atoms can promote the rotation of C—C bonds in graphene and reported graphene growth at graphene edges mediated by a single Cu atom.[18,23] However, only etching activity was observed from Pt atoms at graphene edges. It should be noted that unlike the studies conducted with Fe and Cr atoms which were conducted at room temperature, the studies with Cu and Pt were conducted at the elevated temperatures of 150 or 300 °C. In another in situ TEM study (at room temperature), Au atoms at graphene edges did not exhibit any catalytic behavior (viz., no etching or growth of graphene was observed). In short, these studies show a disparate behavior between elemental atoms and, moreover, show the potential of single-atom catalysts for the edge growth or etching of graphene as well as yielding key insights into the fundamental mechanisms behind such catalytic activity. Here we investigate the catalytic and dynamic activity of tin atoms (monomers and dimers) at graphene edges under electron beam irradiation at room temperature. Tin (Sn)-based SACs have recently been demonstrated to be effective catalysts for different types of chemical reactions. The cheap, non-toxic and eco-friendly properties of Sn make Sn-based catalysts a promising alternative to noble metal catalysts.[7,24–26] Thus, it is important to understand its catalytic activities at the macro- and atomic-scale.

In this in situ HRTEM study, we demonstrate the dynamic catalytic activity (etching and growth) of both mono and binary Sn atoms at the graphene edges under electron beam irradiation at an electron acceleration voltage of 80 kV at room temperature. In so far as we are aware, the dynamic catalytic activity of binary catalyst atoms, which was also investigated in this study, is the first of its kind and, thus, expands our understanding of metal atoms as catalysts.

2. Results and Discussion

2.1. Monomer Activity

Sn atoms and clusters deposited over a graphene monolayer was used to evaluate the behavior of Sn atoms along a graphene edge. The deposition of Sn was achieved by the sublimation and decomposition of tin acetylacetonate (acac) over graphene residing on a standard lacey carbon molybdenum TEM grid in vacuum (≈10^{-6} mbar) at an elevated temperature (300 °C). [16,26] Thereafter, the specimen was cooled and removed from the vacuum sealed vial and then immediately placed in a TEM. The specimen was then exposed to an electron beam shower for 2–20 min (dose ≈ 6×10^3 A m^{-2}), which removes the excess amorphous carbon that forms on the graphene surface during the annealing step. The electron beam shower also helps complete any incomplete decomposition of the Sn acac.[27] Energy dispersive spectroscopy (EDS) was implemented to confirm the presence of Sn. (Figure S1g in the Supporting Information). In addition, to confirm that single atoms at the graphene edge are solely Sn atoms, we used local electron energy loss spectroscopy (EELS). A typical example provided in Figure S1h in the Supporting Information shows the EELS data collected from the red region shown in Figure S1b in the Supporting Information. The study confirms that the graphene comprises C as indicated by the C K-edge at 284 eV, and Sn as indicated by the Sn $M_{4,5}$-edge at 485 eV which arises from the edge atoms (dark contrast) at a graphene pore. No other elements were detected. Moreover, to further confirm that Sn atoms are observed in our TEM study, relative intensity measurements (relative to graphene) for single-atom Sn, Si, and Cu atoms were conducted since Si and Cu are the two most likely contaminants. The experimental data were compared to image simulations, as presented in Figure S1c–f,i in the Supporting Information. These data are also in agreement with the analytical studies confirming that the observed atoms at graphene edges in our study are Sn atoms.

We now turn to the in situ dynamic studies of a single (monomer) and double (dimer) Sn atom/s systems at graphene edges. We begin with the case of the monomer systems. **Figure 1** shows the catalytic growth of graphene by a single Sn atom as it diffuses along the graphene edge under electron beam irradiation (typical dose = 1.8×10^6 A m^{-2}). The atoms at the graphene edge did not migrate in any specific direction along the edge during the process. Panels (a) and (b) show the single-atom dynamic behavior at $t = 0$ and 2.5 s, respectively. Supporting image simulations and stick-and-ball models are provided in Figure 1e–h in the Supporting Information respectively. The Sn atom is initially located in a valley at a zigzag edge; subsequently, it migrated after 2.5 s to a pentagonal C structure that was deficient in one C atom, while four C atoms (marked as the red balls in Figure 1d,h were inserted into graphene to complete the formation of three hexagons (marked by the green arrows). The formation of these new hexagonal structures demonstrates the catalytic ability of a single Sn atom for the growth of graphene. Another example of this growth process, with additional micrographs to highlight the newly inserted C atoms upon Sn migration during catalytic growth can be seen in **Figure 2**. Panels (a) and (b) show the HRTEM image of a single Sn atom's dynamic behavior at $t = 0$ and 3 s, respectively. Supporting image simulations and stick-and-ball models (Figure 2e–h respectively) of Sn atoms at the graphene edge help to clearly demonstrate and confirm this growth process. Initially, the Sn atom sits in a corner of a zigzag edge probably with two Sn—C bonds; subsequently (after 3 s), it migrates to

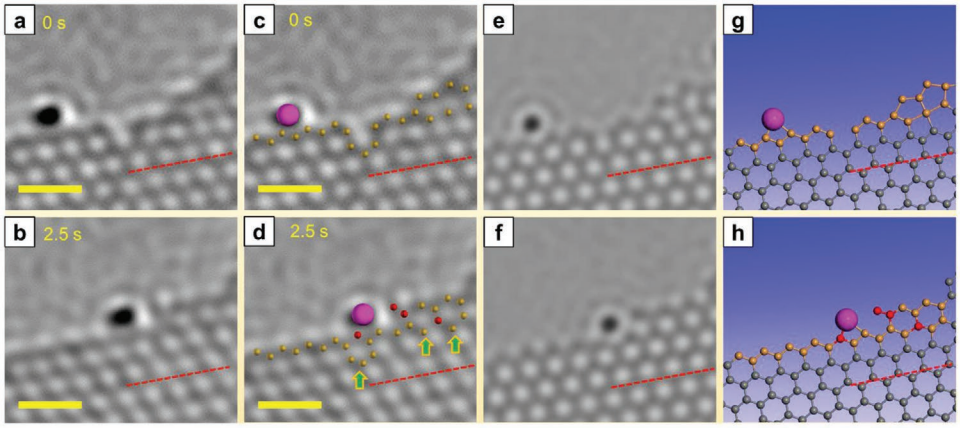

Figure 1. Catalytic growth (C incorporation) by a diffusing Sn monomer at a graphene edge under electron beam irradiation. a,b) HRTEM images showing the catalytic activity. c,d) HRTEM images with added ball models to aid viewing of C atom incorporation. e,f) Image simulations of the growth process. g,h) Complete stick-and-ball models. Note: The rose-red ball and yellow ball indicate the Sn and C atom, respectively. The red balls and green arrows signify the newly inserted C atoms and new forming new hexagonal structures. The red dashed line is the reference line. Dose $\approx 1.8 \times 10^6$ A m^{-2}. All scale bars are 0.5 nm.

form a fully reconstructed zigzag edge[28,29] by incorporating eight C atoms. These are marked as red balls and highlighted with a circle in Figure 2d, and h). This further example again confirms the catalytic potential of Sn atoms to grow graphene at room temperature under electron irradiation. A further example is provided in Figure S2 in the Supporting Information. This is consistent with results from Cr, Fe, Cu single atoms catalytically growing graphene atoms.[15,16,18] In all these cases, the C source for the growth is from hydrocarbon contaminants in the TEM chamber.[30]

We also observed cases where etching of the graphene edge occurred as a single Sn atom (monomer) diffused along the edge. An example is presented in **Figure 3**, which shows HRTEM images of the process (Figure 3a–c), HRTEM images with partial ball models to aid viewing (Figure 3d–f), image simulations (Figure 3g–i)) and stick and ball models of the catalytic etching activity. Panels (a–c) show the single-atom dynamic behavior at $t = 0$, 1.5, and 6 s, respectively. In the first configuration panel (a), an Sn atom embedded in the corner is almost enclosed by the surrounding atoms. It appears to have substituted two C atoms and built three Sn—C bonds at the graphene edge. Subsequently, the atom migrates to a quadrilateral C structure with a dangling C atom after 1.5 s. During this step, four C atoms are removed (represented by blue circles in Figure 3e). The image simulations and stick-and-ball models (Figure 3h,k) of diffusing monomer at the graphene edge help elaborate the etching process. In the third image, panel (c), The Sn atom has migrated to a new position, and in the process, further C atoms have been removed (represented by blue circles in Figure 3f). The

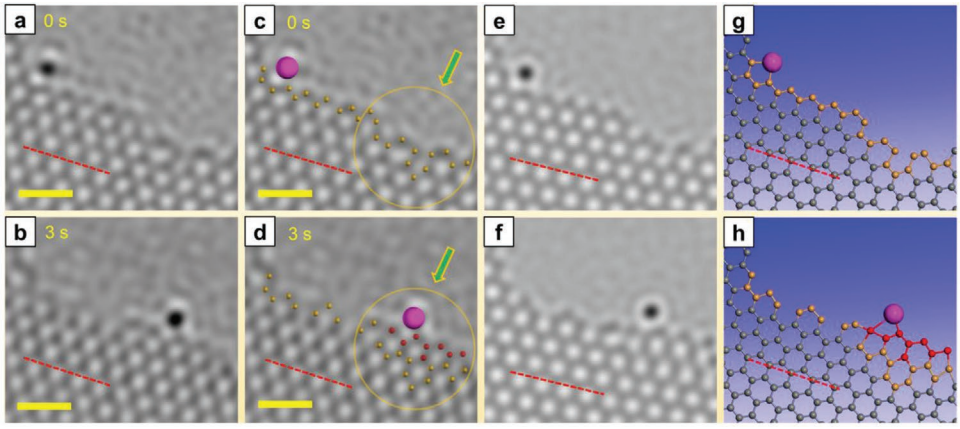

Figure 2. Catalytic growth (C incorporation) by a diffusing Sn monomer at a graphene edge under electron beam irradiation forming three lateral new hexagons. a,b) HRTEM images showing the catalytic activity. c,d) HRTEM images with added ball models to aid viewing of C atom incorporation. e,f) Image simulations of the growth process. g,h) Complete stick-and-ball models. Note: The rose-red ball and yellow ball indicate the Sn and C atom, respectively. The red balls and green arrows signify the newly inserted C atoms and new forming new hexagonal structures. The red dashed line is the reference line. Dose $\approx 1.8 \times 10^6$ A m^{-2}. All scale bars are 0.5 nm.

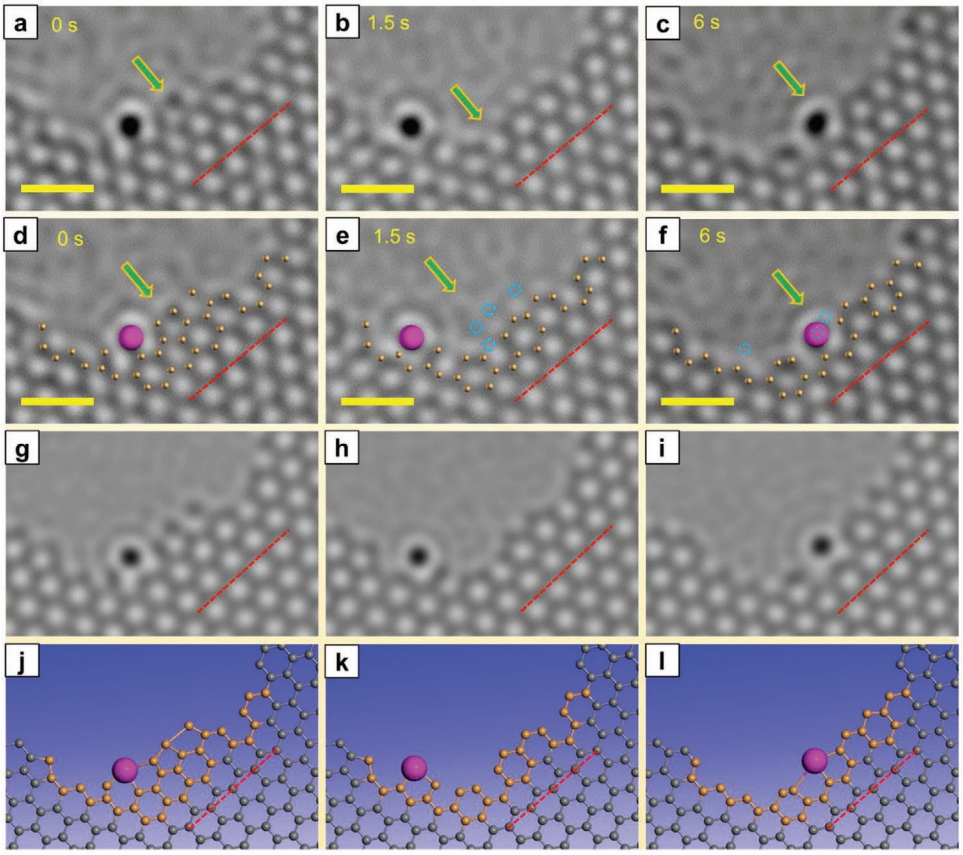

Figure 3. Catalytic etching of graphene by a single Sn atom (monomer) at a graphene edge under electron irradiation. a–c) HRTEM images showing the catalytic activity. d–f) HRTEM images with partial ball models to aid viewing. g–i) Image simulations of the growth process. j–l) Complete stick-and-ball models. The rose-red and yellow balls indicate the Sn and C atoms, respectively. The blue circle and green arrows indicate removed C atoms. The red dashed line is the reference line. Dose ≈ 1.8×10^6 A m^{-2}, and all scale bars are 0.5 nm.

presented example demonstrates single Sn atom etching of graphene. Etching by other elemental atoms has also been observed in other studies, for example, Fe, Si, Au, and Pt atoms. [15,17,19,21] The etching propensity has been argued to correlate with the binding energies of the edge catalyst atoms with the graphene edge and migration barriers. [19,21] In short, above we have presented examples for both the growth and etching of graphene. It is also worth noting that in a number of instances both growth and etching can be observed to occur together in an image series observing the diffusion of Sn monomer atoms at a graphene edges as for example demonstrated in Figure S3 in the Supporting Information. This phenomenon is discussed later on.

To gain further insight into the dynamic behavior of single Sn atoms (monomers) at graphene edges, we examined their frequency for different termination configurations and their relative energies. The different observed configurations are provided in **Figure 4**I–III as HRTEM micrographs, image simulations and stick & ball structures, respectively. We also examine the statistical frequency of the Sn atoms at these seven typical configurations (Figure 4a–g) for a typical electron beam dose of 1.8×10^6 A m^{-2}. The frequency for each configuration decreases from a to g (see Figure 4A). The most frequent atomic structure Figure 4a is the configuration where a Sn atom embeds itself into a graphene edge and builds two Sn—C bonds, forming a pentagonal structure at an armchair edge. The frequency of this pentagonal structure was 10 times that of the hexagonal structure at a zigzag edge (Figure 4g). The second most frequent observation was for an Sn atom in a "large" armchair where two armchair sites merge forming a single larger configuration (Figure 4b). These frequent observations of the Sn atoms in armchair configurations are concomitant with observations for Cr atoms at graphene edges.[31] The third most frequent structural observation is an Sn atom residing at a zigzag configuration. Thereafter several structures, which we term, semi-substitutional configurations (Figure 4d–g). To understand the structural preference, we further investigated the relative energies (ΔE) of these structures using density functional theory (DFT) calculations (Figure 4B). The DFT results showed that the relative energy of the pentagonal structure at an armchair edge (Figure 4a) was the lowest (which we set to 0 eV for relative energy values for all other configurations to be set against). The relative energies for the different configurations increase in a manner very similar to the observed frequency of observation. This indicates that, as compared to the armchair configuration, all other Sn atom configurations require more energy. There is an approximate correlation between the frequency for the different structural formations for Sn atom termination

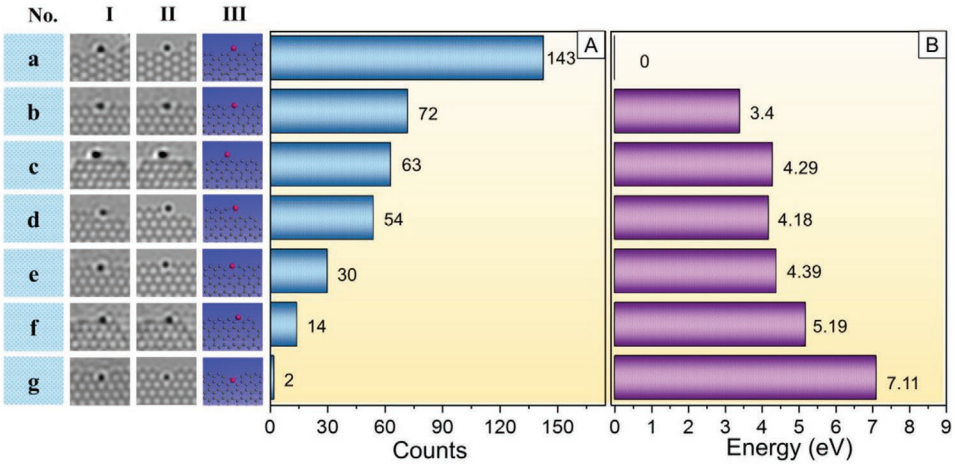

Figure 4. Different configuration frequencies and relative energies (ΔE) of Sn at different graphene edge terminations. A) Plot of the experimentally observed frequency of Sn for different graphene edge terminations. A total of 378 atomic configurations were counted to check the configuration frequencies. B) The relative energies (ΔE) of Sn for different graphene edge terminations. I–III) HRTEM images, image simulation, and stick-and-ball model, respectively, for the different configurations in (a–g). The relative energy (ΔE) is defined as $\Delta E = E_{tot}(X) + n\,E_C - E_{ref}$, where $E_{tot}(X)$, E_C, and E_{ref} represent the total energy of X configuration, a C atom in graphene, and the reference configuration which has the lowest energy, respectively. Here, n indicates the number of C atoms short of those of the reference configuration.

at graphene edges and their energy (relative to armchair termination).

2.2. Dimer Activity

We also observed very interesting activity when two Sn atoms (dimers) diffuse under electron irradiation. It is not only exciting in terms of their behavior but also that, in so far as we are aware, such dimer activity at graphene edges has not been reported previously.

Figure 5 shows an Sn dimer at a monolayer graphene edge. Under the electron beam irradiation, the atoms migrate to different edge locations. Panels (a–c) show the binary atom dynamic behavior at $t = 0$, 0.5, and 1 s, respectively. The possible motion of the atoms is unclear and could be interpreted as a hopping process or a shuffling process. The two possible dynamic motion modes (hopping and shuffle) are shown in Figure 5g–l), respectively. In the hopping process, the first Sn atom bypasses the second Sn atom and jumps to a pentagonal C structure that was deficient by one C atom after 0.5s (see Figure 5g–h).

Subsequently, the second Sn atom bypasses the first and jumps to another pentagonal structure after 1 s (see Figure 5h,i). In the shuffle scenario, the second Sn atom moves to a pentagonal structure, and the first atom translocates to the original position of the second atom (see Figure 5j,k). Subsequently, the second Sn atom again shifts to another pentagonal structure, and the first atom shuffles to the original position of the second atom again (see Figure 5k,l). Further examples of this Sn dimer behavior are provided in Figure S4 in the Supporting Information. However, these findings raised the question: how can one determine whether the process involves the hopping or shuffling of Sn? To determine this, we examine some remarkable HRTEM micrographs and also implement theoretical energy profile studies. We begin with a series of in situ HRTEM studies that capture the dynamic process of the two Sn atoms before, during and after their seemingly parallel diffusion along the graphene edge (e.g., **Figure 6**). The image capture time is 0.5 s. Figure 6a–c shows the binary atoms dynamic behavior at $t = 0$, 0.5, and 1 s, respectively. Initially, the two Sn atoms were incorporated into an armchair edge position next to each other (panel (a)). In the subsequent micrograph, there now appear to four atoms at the graphene edge as if two new atoms have appeared to the left of the original pair of Sn atoms (panel (b)). In the final image, only the left pair is seen (panel (c)). However, it is strikingly obvious that the intensity of the "apparent" four atoms in panel (b) is less than the pair of atoms in panels (a) or (c). One can also quantify the intensities (relative to graphene) for each of the panels (a–c). The relative intensity values are presented in panels (g,h,I) respectively. The values for the Sn atoms in panels (a) and (c) are around 5, while for the panel (b) the four atoms relative intensities are about half. This is attributed to the initial binary atoms that have moved during the image in panel (b) being acquired (0.5 s). Moreover, no streaking of the atom was observed in the acquisition of the image in panel (b). Streaking can occur when the atom motion is sufficiently slow during the image acquisition so that the atoms position is captured across various spatial locations, as for example demonstrated in a work looking at the catalytic action of Fe atoms at graphene edges.[15] In the micrograph in panel (b), no streaking is observed such that only the initial and final position of the atoms is captured in the image. This indicates the transition time for the atoms during diffusion is rather fast, viz., no streaking is observed.

In short, panel (b) shows the binary atoms firstly as a pair to the right (as initially seen in panel (a)) and then as a pair to the left (as later seen in panel (c)). This points to the movement of the binary atoms being from the right to the left as a pair in some manner, as depicted in panels (d–f).

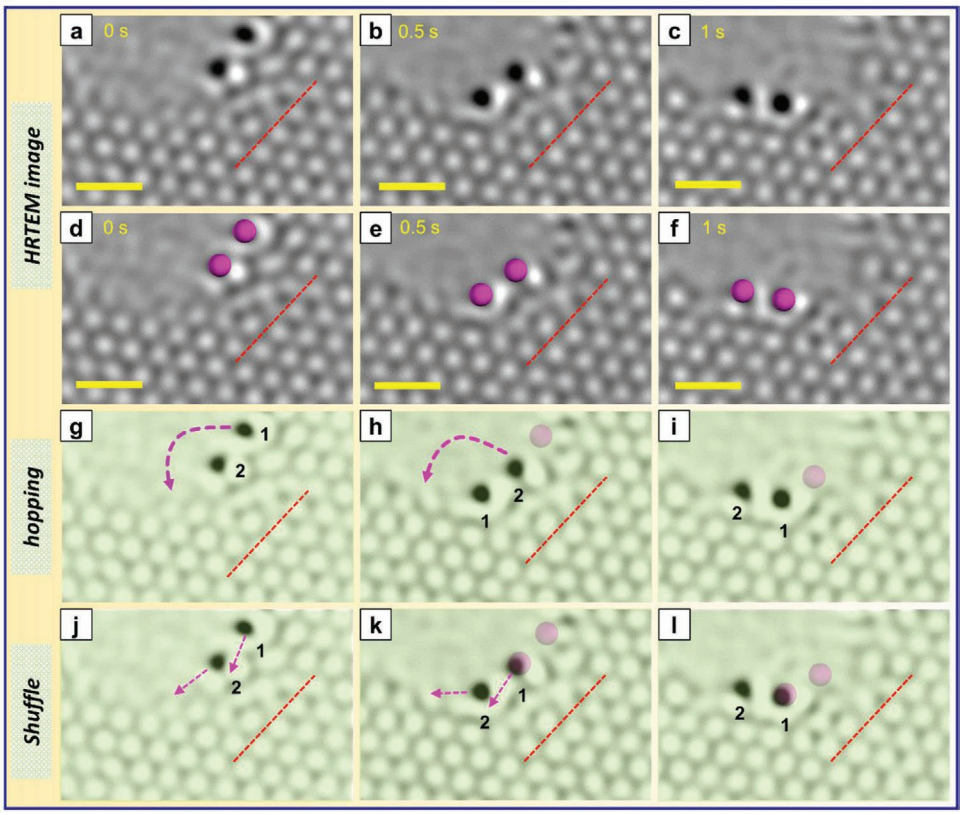

Figure 5. Activity of an Sn dimer along a graphene edge under electron irradiation. a–c) HRTEM images showing binary atoms activity. d–f) HRTEM images with partial ball models to aid viewing. g–i) HRTEM images showing possible atom hopping activity. j–l) HRTEM images showing possible atom shuffle activity. The rose-red balls indicate the Sn atom, and the translucent rose-red balls represent the previous positions of the Sn atom. Dose $\approx 1.8 \times 10^6$ A m^{-2}, and all scale bars are 0.5 nm.

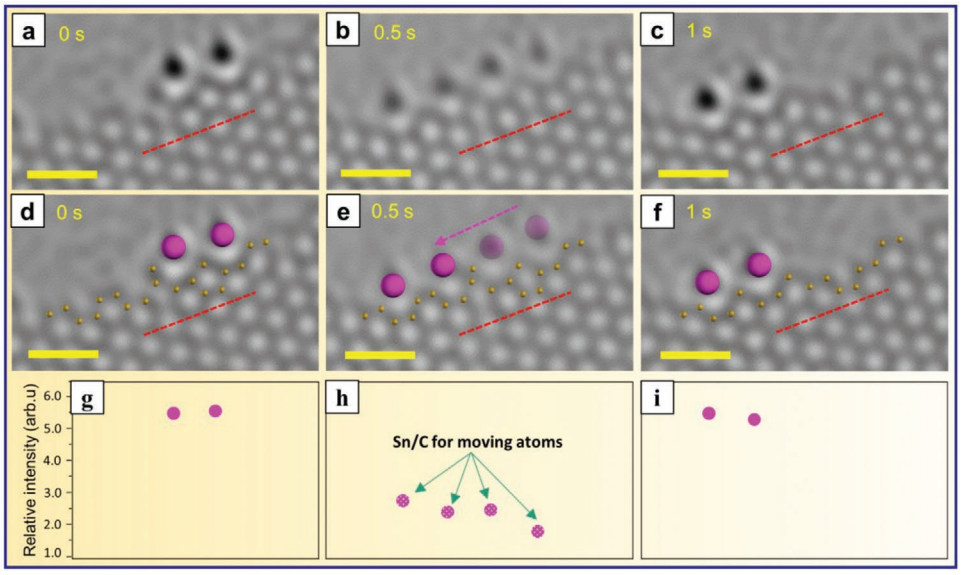

Figure 6. Shifting activity (with intermediate capture) of two Sn atoms (dimer) at a graphene edge under electron irradiation. a–c) HRTEM images showing the shifting activity. d–f) HRTEM images with partial ball models to aid viewing. g–i) Comparison of the relative intensity ratios for Sn atoms derived from the HRTEM images. The rose-red balls indicate the Sn atoms. The translucent rose-red balls represent the previous position of the Sn atom. The red dashed line is the reference line. Dose approx. 1.8×10^6 A m^{-2}, and all scale bars are 0.5 nm.

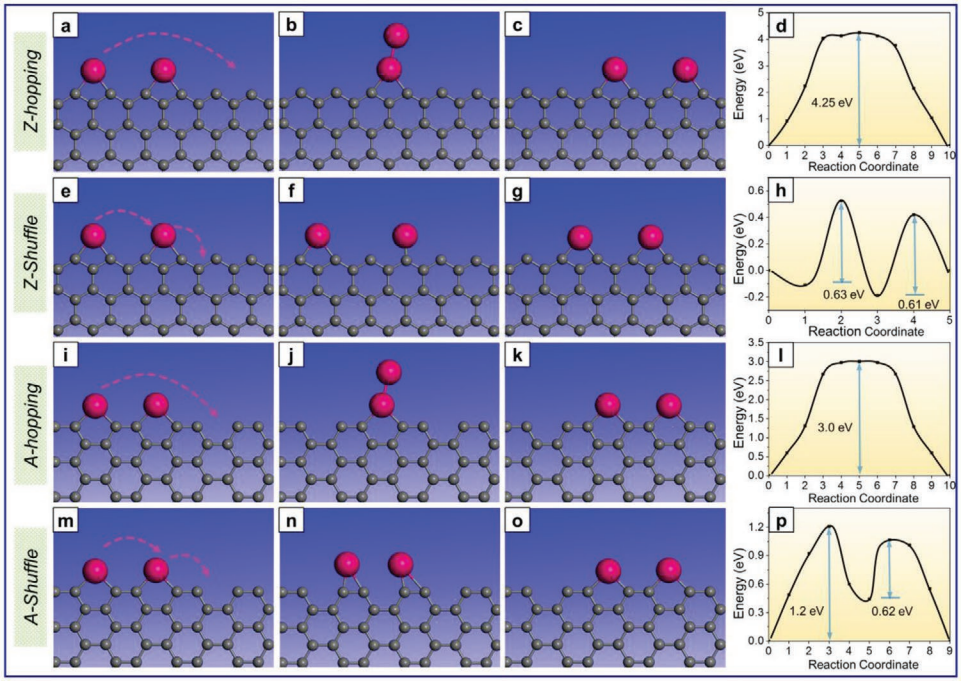

Figure 7. a–c) The NEB calculated initial, transition, and final state configurations of Sn atoms in a hopping process at zigzag edge terminations and d) the related energy profile. e–g) The NEB calculated initial, transition, and final state configurations of Sn atom shuffle process at zigzag edge terminations and h) the related energy profile. i–k) The NEB calculated initial, transition, and final state configurations of the Sn atom hopping process at armchair edge terminations and l) the related energy profile. m–o) The NEB calculated initial, transition, and final state configurations of Sn atom the shuffle process at armchair edge terminations and p) the related energy profile.

We also investigated the catalytic behavior of the dimer systems at graphene edges. The study showed that dimer diffusion at graphene edges can lead to growth, etching and at times both can be observed in a single image series. Some examples are provided in Figures S4–S7 in the Supporting Information.

To better identify the Sn binary atoms diffusion mechanism at the graphene edge, we calculated the energy profiles for two possible pathways of two Sn atoms at both armchair and zigzag edges using the nudged elastic band (NEB) method. [32] The two pathways we examined were a hopping process and a shifting scenario, as shown in **Figure 7**, for the two edge configurations. The transition state (TS) for the hopping processes involves one Sn atom moving (hopping) over another (see Figure 7a–c,i–k). The corresponding energy barriers were ≈4.3 eV (Figure 7d) and 3.0 eV (Figure 7i), for the zigzag and armchair configurations, respectively. In contrast, the transition state (TS) for the shifting process involves an Sn atom shuffle activity in which one atom leads the diffusion in one direction, rapidly followed by the second atom. These consecutive diffusion steps suggest a shuffle process. The energy barriers for the shuffle process are ≈0.63 eV for the zigzag edge and ≈1.20 eV for the armchair edge. It is worth noting that in the TS of the armchair edge, the two Sn atoms are still paired, in contrast to the step-wise diffusions at the zigzag edge. The significantly lower energies for the shuffle process as compared to the hopping process indicate that the shuffle process is the most likely mechanism by with the atoms move/diffuse at graphene edges as a pair (dimer), as we often observed experimentally (also see Figures S4 and S5 in the Supporting Information). However, in not all instances did we observe Sn dimers at graphene edges to exhibit a parallel shift (shuffle) of the atoms. In some cases, the atoms go in separate directions (see Figures S6 and S7 in the Supporting Information) viz., the dimer collapses to two monomers. To better quantify these observations, we conducted a detailed statistical analysis of the dimers diffusion at graphene edges whilst under electron irradiation. The data are shown in **Figure 8**. We observed 48 Sn dimers at graphene edges. Of these, 38 shifted as a pair and 10 shifted apart (collapse to two monomers). This clearly indicates that paired atoms have a strong propensity (four times more likely) to diffuse together (shuffle) as compared to separate, viz., some attractive interaction must exist. To better comprehend intriguing aspects, we first gather more detailed statistics on the Sn dimers for different graphene edge configurations (armchair, zigzag and chiral [mix]) and their movement as a pair (shuffle) or separating (split). The data are presented in Figure 8a. For binary atoms following a coupled or shuffle translation, armchair configurations overwhelmingly dominate, followed by chiral (mixed) edges, and the fewest TS occur for armchair configurations. In terms of the dimers collapsing to two monomers (i.e., splitting), this occurs mostly for zigzag configurations and less so at mixed or armchair configurations. In short, the data point to an atom or both atoms in a binary pair at a graphene edge, that remain as a pair upon edge diffusion, favoring the involvement of at least one graphene armchair edge structure. To better understand this remarkable interaction of the Sn dimers, we calculated the relative binding energies (ΔE_{bind}) for Sn monomers and Sn dimers at armchair and zigzag graphene edges (see Methods). ΔE_{bind} are

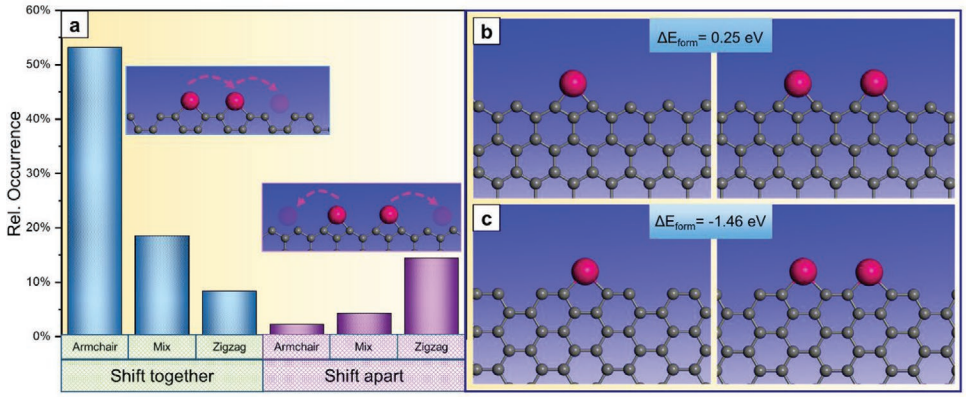

Figure 8. a) The relative occurrence diffusion behavior (as a pair or splitting) for different Sn dimer/edge configurations under electron irradiation. b) The optimized configurations of Sn monomers and dimers at a zigzag edge. c) The optimized configurations of Sn monomers and dimers at an armchair edge.

0.25 eV for a zigzag edge (Figure 8b) and –1.46 eV for armchair edge (Figure 8c), respectively. The data reveals two interesting aspects. In the first, the positive relative binding energy indicates that the zigzag edge favors individual Sn atoms rather than dimers and so, paired atoms (dimers) are likely to separate on diffusing, exactly as we observe experimentally. Secondly, in the case of Sn single and binary atoms at armchair terminations, the binding energy for Sn pairs (dimers) is significantly lower than for a single Sn atom. This explains why when the binary atoms are on armchair sites they prefer to synchronize their diffusion such that as soon as one atom moves, the second will follow in the same direction (shuffle) so as to minimize its energy. This explains why, experimentally, we see synchronized diffusion of binary atoms in a dimer so often and moreover, why this is found predominantly the case at armchair sites.

We now turn to the discussion as to why Sn catalyst (monomers and dimers) at the graphene edge can etch and grow graphene under exactly the same imaging conditions. In other words, both catalytic actions occur with the same imaging dose and electron acceleration energy. While it may be that dose and electron acceleration energy could affect the catalytic action of the Sn atoms in terms of "forcing" a Sn atom to preferentially grow or etch graphene, under our imaging conditions, this is obviously not an argument that can explain both behaviours occuring simultaneously in an image series where the imaging conditions are identical. To understand why an Sn atom, under our imaging conditions, prefers growth or etching we look to the case of gold catalysts growing co-axial B/BO_x nanowires under electron beam irradiation. In particular, once a B/BO_x co-axial nanowire has been grown, the Au clusters, upon extended irradiation, start to etch the B core of the as-grown B/BO_x nanowires leaving a BO_x nanotube. This occurs because initially there is a sufficient supply of B atoms for the nanowire growth. Later, once the external supply of B species is depleted the Au catalyst cluster continues with exactly the same catalytic action, but now uses B from the as-grown B nanowires, thus, in essence etching the core B nanowire leaving only the outer caseing, the BO_x outerlayer (now a hollow tube).[33] In our study, we propose the same argument, namely, the Sn atm does not change its catalytic action per se. In fact, the atoms follow exactly the same catalytic action when growing or etching a graphene edge. The only difference lies in where it obtains a carbon atom and where it then deposits that captured carbon atom. This is illustrated in **Figure 9**a. In the first catalytic action on the left, a C atom from vacuum is captured by the Sn catalyst atom and then deposited at the graphene edge and represents growth. In the right example a C atom from the graphene edge is captured by the Sn catalyst atom and the C is then ejected to the vacuum and this represents etching. However, the Sn atoms sees no difference in its catalytic action. It simply captures a C atoms and then releases/deposits it elsewhere. However, the capture of a C atom from a graphene edge, as compared to C from the vacuum, will be a more costly process energetically. Thus, by controlling the supply of C atoms one can control the growth or etching of the Sn atom. Future studies with environmental TEM experiments should help confirm this concept. The catalytic process of an Sn atom in the presence of a high C supply in the vacuum (for graphene growth) is shown schematically in panel (b). In panel (c), the schematic shows the scenario where there is a lack of C atoms in the vacuum, thus, C atoms from the graphene edges are consumed (etching). Finally, in panel (d), the schematic shows the scenario where only a limited supply of C atoms are present in the vacuum and thus, both growth and etching are observed.

3. Conclusions

The diffusion behaviors of Sn monomers and dimers at monolayer graphene edges under electron irradiation were investigated in situ. Sn monomer diffusion exhibited both C atom removal and incorporation, viz., single Sn atom catalytic etching and growth of graphene, respectively. To understand the structural preferences, we observed experimentally in terms of the Sn atom-graphene edge termination (monomer interfacing), we investigated the relative energies (ΔE) of these monomer interfacing structures using DFT calculations. The DFT and experimental data are consistent and show an approximate correlation between the frequency for the different structural formations for Sn atom termination at graphene edges and their energy (relative to armchair termination). We also observed the dynamic diffusion of Sn atom pairs (dimers) at graphene

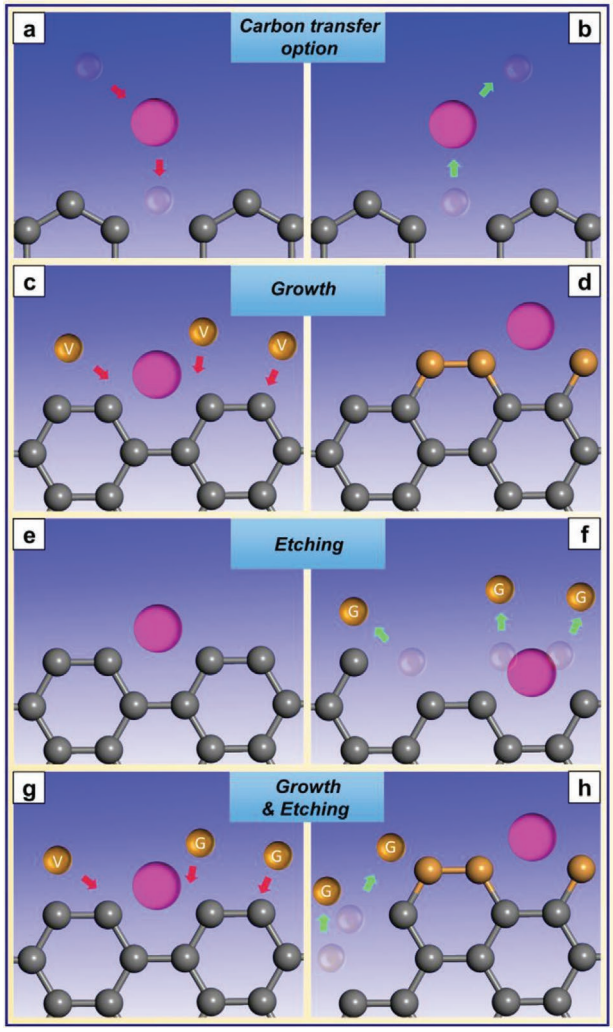

Figure 9. Schematic figures demonstrating: a) Left: C capture from vacuum by an Sn atom and subsquebt release to a graphene edge (growth). Right: C capture from a graphene edge and release to the vacuum (etch). b) Schematic showing the catalytic growth of graphene from a single Sn atom with a plentiful C supply in vacuum. c) Schematic showing the catalytic etching of graphene from a Sn atom due to a lack of C atoms in vacuum. d) Schematic showing catalytic growth and etching of graphene at the same time with a limited C supply in vacuum. The rose-red balls indicate a Sn atom. The orange balls with red arrows indicate newly inserted C atoms. The orange balls with green arrows indicate captured/removed C atoms. The translucent orange balls represent the previous positions of the C atoms. The V symbol and G symbol marked on the C atom represent if the carbon atoms were captured from vacuum or graphene, respectively.

edges, which, in so far as we are aware, is the first such report. Experimental and supporting theoretical investigations revealed a synchronized edge dependence of the diffusing atoms in Sn dimers. Electron irradiation driven diffusion of Sn atom pairs in a dimer occurs in a shuffle process (as opposed to a hopping action) and, moreover, the shuffle process depends on the graphene edge termination. Atom pairs (dimers) involving an armchair graphene edge configuration tend to diffuse with a synchronized shuffling (step-wise shift) action, while dimer diffusion at zigzag edge terminations show a strong propensity do to collapse the dimer with each atom diffusing in opposite directions (monomer formation). Moreover, the data points to the availability of an external C feedstock dictating if a Sn catalyst atom grows or etches graphene, however, from the Sn atoms perspective, there is no difference in its catalytic action, it simply depends where the C feedstock arrives from, namely, the vacuum or the graphene edge. This new insight to the catalytic action of single atoms at graphene edges as well as the remarkable Sn dimer observations and the resultant new and fundamental understanding of paired metal atoms at graphene edges provide further research directions for the catalytic effects of monomer and dimer systems for crystal growth.

4. Experimental Section

Sample Fabrication and Preparation: The Sn material was deposited over a graphene monolayer, which was used to evaluate the behavior of Sn atoms along a graphene edge. The graphene base was prepared by thermal chemical vapor deposition (CVD) over a Cu foil, as described in previous studies.[34,35] The graphene layer was then transferred onto standard lacey carbon molybdenum TEM grids by spin coating with polymethyl methacrylate (PMMA). Subsequently, the Cu foil was etched away using ammonium persulfate. The TEM grid with the transferred graphene layer was placed in a quartz vial with a nominal amount of Sn acetyl acetonate (acac) for the deposition of the Sn atoms on the graphene. The vial was then evacuated to $\approx 10^{-6}$ mbar, sealed, and heated to 300 °C for 12 h. The sublimation and decomposition of the Sn acac left behind a nominal amount of Sn atoms on the graphene surface. This specimen was exposed to an electron beam shower for 2–20 min (current ≈9 nA; current density $\approx 6 \times 10^3$ A m^{-2}) by TEM after the deposition of the Sn atoms. The specimen was annealed under vacuum ($<10^{-6}$ mbar) overnight at 250 °C prior to the in situ TEM experiments.

TEM Studies: The TEM (Titan^3, FEI Company (Thermo Fisher Scientific), Oregon, USA) in the experiment was equipped with a monochromator and a spherical aberration corrector for the primary objective lens. The electron acceleration voltage was 80 kV.

Multislice TEM Image Simulation: The multislice high-resolution image simulations were conducted using an electron microscopy simulation software (JEMS, Dr. P. Stadelmann, Jongny, Switzerland). All the simulation parameters were similar to those used in TEM. The electron acceleration voltage and energy spread were 80 kV and 0.2 eV, respectively. The coefficients of chromatic aberration (Cc) and spherical aberration (Cs) were set to 1 mm and 1 µm, respectively. The focuses were typically 2 and 3 nm, with a defocus spread of 2 nm.

Density Functional Theory (DFT) Calculations: First-principles DFT calculations were performed using the projector-augmented wave (PAW) method[36] and the Perdew-Burke-Ernzerhof (PBE) exchange-correlation functional,[37] as implemented in the Vienna Ab-initio Simulation Package.[38,39] The plane-wave basis set with a cutoff energy of 550 eV was adopted in optimization calculations. The Brillouin zone was sampled using a $1 \times 3 \times 1$ mesh. The relative binding energy ΔE_{bind} is defined by the formula $\Delta E_{bind} = E_{bind/2Sn} - 2 \times E_{bind/1Sn}$. The binding energy ($E_{bind}$) is calculated by the formula: $E_{bind} = E_{total} - E_{gra} - n \times E_{Sn}$, where E_{total}, E_{gra}, and E_{Sn} represent the total energy of Sn at graphene edge, graphene without Sn and one Sn atom. Here, n is the number of Sn atoms.

Supporting Information

Supporting Information is available from the Wiley Online Library or from the author.

Acknowledgements

X.Y., H.Q.T., and H.H. contributed equally to this work. This work was supported by the National Natural Science Foundation of China (Grant Nos. 52071225, 51676154, and 11874044) and the Czech Republic by ERDF "Institute of Environmental Technology-Excellent Research" (No. CZ.02.1.01/0.0/0.0/16_019/0000853). M.H.R. appreciates the Sino-German Research Institute for its support (project: GZ 1400). H.Q.T. thanks the Alexander von Humboldt foundation for its support through an Alexander von Humboldt Fellowship. All authors contributed to the manuscript and provided their approval to the final version of the same.

Open access funding enabled and organized by Projekt DEAL.

Conflict of Interest

The authors declare no conflict of interest.

Data Availability Statement

Research data are not shared.

Keywords

dimer, graphene, monomers, single atom catalysts, tin, transmission electron microscopy

Received: May 7, 2021
Revised: June 21, 2021
Published online: July 6, 2021

[1] K. Qi, M. Chhowalla, D. Voiry, *Mater. Today* **2020**, *40*, 173.
[2] M. Fan, J. Cui, J. Wu, R. Vajtai, D. Sun, P. M. Ajayan, *Small* **2020**, *16*, 1906782.
[3] B. Zhang, T. Fan, N. Xie, G. Nie, H. Zhang, *Adv. Sci.* **2019**, *6*, 1901787.
[4] C. Rivera-Cárcamo, P. Serp, *ChemCatChem* **2018**, *10*, 5058.
[5] B. Zhang, H. Asakura, J. Zhang, J. Zhang, S. De, N. Yan, *Angew. Chem., Int. Ed. Engl.* **2016**, *55*, 8319.
[6] J. Li, M. F. Stephanopoulos, Y. Xia, *Chem. Rev.* **2020**, *120*, 11699.
[7] S. K. Kaiser, Z. Chen, D. Faust Akl, S. Mitchell, J. Perez-Ramirez, *Chem. Rev.* **2020**, *120*, 11703.
[8] L. Liu, A. Corma, *Chem. Rev.* **2018**, *118*, 4981.
[9] Q. Zhang, J. Guan, *Adv. Funct. Mater.* **2020**, *30*, 2000768.
[10] H. Fei, J. Dong, D. Chen, T. Hu, X. Duan, I. Shakir, Y. Huang, X. Duan, *Chem. Soc. Rev.* **2019**, *48*, 5207.
[11] G. Sun, Z. J. Zhao, R. Mu, S. Zha, L. Li, S. Chen, K. Zang, J. Luo, Z. Li, S. C. Purdy, A. J. Kropf, J. T. Miller, L. Zeng, J. Gong, *Nat. Commun.* **2018**, *9*, 4454.
[12] T. Zheng, K. Jiang, N. Ta, Y. Hu, J. Zeng, J. Liu, H. Wang, *Joule* **2019**, *3*, 265.
[13] H. Yan, H. Cheng, H. Yi, Y. Lin, T. Yao, C. Wang, J. Li, S. Wei, J. Lu, *J. Am. Chem. Soc.* **2015**, *137*, 10484.
[14] L. L. Patera, F. Bianchini, C. Africh, C. Dri, G. Soldano, M. M. Mariscal, M. Peressi, G. Comelli, *Science* **2018**, *359*, 1243.
[15] J. Zhao, Q. Deng, S. M. Avdoshenko, L. Fu, J. Eckert, M. H. Rummeli, *Proc. Natl. Acad. Sci. USA* **2014**, *111*, 15641.
[16] H. Q. Ta, L. Zhao, W. Yin, D. Pohl, B. Rellinghaus, T. Gemming, B. Trzebicka, J. Palisaitis, G. Jing, P. O. Å. Persson, Z. Liu, A. Bachmatiuk, M. H. Rümmeli, *Nano Res.* **2018**, *11*, 2405.
[17] W. L. Wang, E. J. Santos, B. Jiang, E. D. Cubuk, C. Ophus, A. Centeno, A. Pesquera, A. Zurutuza, J. Ciston, R. Westervelt, E. Kaxiras, *Nano Lett.* **2014**, *14*, 450.
[18] E. Kano, A. Hashimoto, M. Takeguchi, *Appl. Phys. Express* **2017**, *10*, 025104.
[19] H. Wang, Q. Feng, Y. Cheng, Y. Yao, Q. Wang, K. Li, U. Schwingenschlögl, X. X. Zhang, W. Yang, *J. Phys. Chem. C* **2013**, *117*, 4632.
[20] N. Cheng, L. Zhang, K. Doyle-Davis, X. Sun, *Electrochem. Energy Rev.* **2019**, *2*, 539.
[21] H. Wang, K. Li, Y. Cheng, Q. Wang, Y. Yao, U. Schwingenschlogl, X. Zhang, W. Yang, *Nanoscale* **2012**, *4*, 2920.
[22] K. Yamazaki, Y. Maehara, C.-C. Lee, J. Yoshinobu, T. Ozaki, K. Gohara, *J. Phys. Chem. C* **2018**, *122*, 27292.
[23] E. Kano, A. Hashimoto, T. Kaneko, N. Tajima, T. Ohno, M. Takeguchi, *Nanoscale* **2016**, *8*, 529.
[24] J. L. Zhang, S. Zhao, S. Sun, W. Wang, Z. Ma, X. Lian, Z. Li, W. Chen, *J. Phys. Chem. Lett.* **2021**, *12*, 745.
[25] F. Luo, A. Roy, L. Silvioli, D. A. Cullen, A. Zitolo, M. T. Sougrati, I. C. Oguz, T. Mineva, D. Teschner, S. Wagner, J. Wen, F. Dionigi, U. I. Kramm, J. Rossmeisl, F. Jaouen, P. Strasser, *Nat. Mater.* **2020**, *19*, 1215.
[26] X. Yang, H. Q. Ta, W. Li, R. G. Mendes, Y. Liu, Q. Shi, S. Ullah, A. Bachmatiuk, J. Luo, L. Liu, J.-H. Choi, M. H. Rummeli, *Nano Res.* **2021**, *14*, 747.
[27] M. H. Rummeli, H. Q. Ta, R. G. Mendes, I. G. Gonzalez-Martinez, L. Zhao, J. Gao, L. Fu, T. Gemming, A. Bachmatiuk, Z. Liu, *Adv. Mater.* **2018**, *31*, 1800715.
[28] P. Koskinen, S. Malola, H. Hakkinen, *Phys. Rev. Lett.* **2008**, *101*, 115502.
[29] K. He, A. W. Robertson, Y. Fan, C. S. Allen, Y.-C. Lin, K. Suenaga, A. I. Kirkland, J. H. Warner, *ACS Nano* **2015**, *9*, 4786.
[30] M. H. Rummeli, Y. Pan, L. Zhao, J. Gao, H. Q. Ta, I. G. Martinez, R. G. Mendes, T. Gemming, L. Fu, A. Bachmatiuk, Z. Liu, *Materials* **2018**, 11.
[31] H. Q. Ta, Q. X. Yang, S. Liu, A. Bachmatiuk, R. G. Mendes, T. Gemming, Y. Liu, L. Liu, K. Tokarska, R. B. Patel, J. H. Choi, M. H. Rummeli, *Nano Lett.* **2020**, *20*, 4354.
[32] G. Henkelman, B. P. Uberuaga, H. Jónsson, *J. Chem. Phys.* **2000**, *113*, 9901.
[33] I. G. Gonzalez-Martinez, S. M. Gorantla, A. Bachmatiuk, V. Bezugly, J. Zhao, T. Gemming, J. Kunstmann, J. Eckert, G. Cuniberti, M. H. Rummeli, *Nano Lett.* **2014**, *14*, 799.
[34] H. Q. Ta, D. J. Perello, D. L. Duong, G. H. Han, S. Gorantla, V. L. Nguyen, A. Bachmatiuk, S. V. Rotkin, Y. H. Lee, M. H. Rummeli, *Nano Lett.* **2016**, *16*, 6403.
[35] M. H. Rümmeli, S. Gorantla, A. Bachmatiuk, J. Phieler, N. Geißler, I. Ibrahim, J. Pang, J. Eckert, *Chem. Mater.* **2013**, *25*, 4861.
[36] P. E. Blochl, *Phys. Rev. B: Condens. Matter Mater. Phys.* **1994**, *50*, 17953.
[37] J. P. Perdew, K. Burke, M. Ernzerhof, *Phys. Rev. Lett.* **1996**, *77*, 3865.
[38] G. Kresse, J. Furthmüller, *Phys. Rev. B* **1996**, *54*, 11169.
[39] G. Kresse, D. Joubert, *Phys. Rev. B* **1999**, *59*, 1758.